

rapid cooling and enhanced recombination do not make contributions. (See Ref. 3 for the comparison of flat- and stepped-target dynamics.) Microdensitometer traces of the spectra for this target configuration are shown in Fig. 4. In Fig. 5, the spatial profiles of the film density of  $Ly\beta$  and  $Ly\gamma$  are shown. The source radiation here is not effectively coupled to the underdense plasma, but the source radiation density is sufficiently strong to lead to inversion. As expected, results are better for the hydrogenic ion pair. Finally, the  $Ly\alpha$  drops off slowly compared to the stepped targets.

From these observations, we conclude that the mechanism leading to the observed inversion is indeed resonant photoexcitation. Electron density in the region of inversion can be determined from the heliumlike resonance line and the intercombination intensity ratios<sup>3,4</sup> and was found to be somewhat greater than  $10^{20}$   $\text{cm}^{-3}$ . At these densities, the opacity effects are not important for the plasma lengths under consideration. Thus, we have shown experimentally, for the first time, soft x-ray population inversion by resonant photoexcitation. Moreover, population inversions at sufficiently large densities have been obtained in multicomponent plasmas generated by moderate-energy high-intensity lasers. Finally, it is suggested that heliumlike ion combinations apparently are better suited for high

gains at soft x-ray wavelengths when combining the advantages of both photoexcitation and enhanced recombination processes.

The author gratefully acknowledges the continuous guidance and the intensive discussions with Professor M. J. Lubin and Dr. B. Yaakobi, and M. Nabut's help in the preparation of this manuscript. This work was supported by AFOSR No. 77-3189. This work was partially supported by the following sponsors: Exxon Research and Engineering Company, Empire State Electric Energy Research Corporation, and New York State Energy Research and Development Administration.

<sup>1</sup>V. A. Bhagavatula, J. Appl. Phys. **47**, 4535 (1976); A. V. Vinogradov, I. I. Sobelmann, and E. A. Yukov, Sov. J. Quantum Electron. **5**, 59 (1975); B. A. Norton and N. J. Peacock, J. Phys. B **6**, 989 (1975).

<sup>2</sup>M. Galanti, N. J. Peacock, B. A. Norton, and J. Puric, *Proceedings 5th IAEA Plasma-Fusion Conference on Plasma Physics and Controlled Nuclear Fusion Research, Tokyo, Japan, 1974* (IAEA, Vienna, 1974), Vol. II, p. 405; K. G. Whitney and J. Davis, J. Appl. Phys. **45**, 5294 (1974).

<sup>3</sup>V. A. Bhagavatula and B. Yaakobi, Opt. Commun. **24**, 331 (1978).

<sup>4</sup>A. V. Vinogradov, I. Yu. Skobelev, and E. A. Yukov, Sov. J. Quantum Electron. **5**, 630 (1975).

## Extrema of electron density and output pulse energy in a CuCl/Ne discharge and a Cu/CuCl double-pulsed laser

M. J. Kushner and F. E. C. Culick

California Institute of Technology, Pasadena, California 91125  
(Received 25 May 1978; accepted for publication 16 August 1978)

Electron-density measurements have been made in a CuCl/Ne discharge using a  $\text{CO}_2$  laser interferometer. A local maximum followed by a local minimum in electron density have been found to move a higher tube temperature with higher buffer pressure. Extrema in Cu/CuCl double-pulsed laser energy may be correlated with the extrema in electron density. An analysis based on rate equations yields qualitative agreement with measured laser-pulse energies. The results support the idea that ionization of copper is primarily responsible for the decrease of laser output as the tube temperature is increased.

PACS numbers: 42.55.Hq, 52.80.Hc, 42.60.By

The copper laser has been the focus of much interest in recent years as a source of intense nanosecond pulses of optical ( $\lambda = 5106$  and  $5782 \text{ \AA}$ ) radiation.<sup>1-5</sup> Unlike the conventional copper laser which must operate at a tube temperature of about  $1500^\circ\text{C}$ <sup>4</sup> in order to obtain sufficient copper partial pressure from pure copper, the use of copper chloride (CuCl) as a source enables tube temperatures to be within a few degrees of  $400^\circ\text{C}$ . The operation of a Cu/CuCl laser requires at least two discharge pulses separated by tens to hundreds of microseconds. The first pulse dissociates the CuCl into Cu and Cl. The second pulse serves as the pumping pulse. Typical optical-pulse duration is 15–30 ns FWHM with a typical output energy of a few millijoules.

The optical-pulse energy of the double-pulsed

Cu/CuCl laser is a sensitive function of tube temperature, geometry, and discharge characteristics.<sup>6</sup> In particular, the pulse energy exhibits a maximum as a function of tube temperature. Measurements of electron temperature for a fixed tube geometry and buffer-gas pressure<sup>7</sup> revealed that the average electron energy is a minimum at tube temperatures for which the optical-pulse energy is a maximum. In a continuing effort to understand the operation of the Cu/CuCl laser, this letter reports results of electron-density measurements in a CuCl discharge taken with a  $\text{CO}_2$  laser interferometer.

The CuCl discharge was sustained in a 2.54-cm i.d. quartz tube enclosed in a 46-cm-long heater; the electrode spacing was 35.5 cm. The electric discharge con-

sisted of a breakdown pulse (14.4-nF capacitor charged to 5.0 kV) immediately followed by the discharge of a 60- $\mu$ F capacitor charged to 1.5 kV. Copper chloride was placed in a trough running the length of the tube, and the tube was filled with neon. The neon was circulated past NaCl windows to avoid deposition of CuCl on the colder window surfaces. The CO<sub>2</sub> laser interferometer, operating in the TEM<sub>00</sub> mode at 10.6  $\mu$ m, was mounted on a granite table to minimize vibration. The interferometer was constructed according to the descriptions given in Refs. 8 and 9. The electron densities measured with the interferometer were taken as the maximum electron densities occurring during the discharge pulse.

The results of the electron-density measurements are shown in Fig. 1 for four Ne buffer-gas pressures. For a fixed pressure of buffer gas, there appears both a local minimum and maximum in electron density as the tube temperature is changed.<sup>10</sup> The tube temperatures at which these extrema appear increase with increasing buffer-gas pressure. The pattern consists of a maximum followed by a minimum at a higher tube temperature. When Ne alone was placed in the discharge, the local minimum in electron density did not appear. The maximum, however, was found at the same tube temperature for a given pressure as in the CuCl/Ne discharge.

The increase in electron density at low tube temperatures can in part be explained by an increasing  $E/N$  and neon ionization coefficient<sup>11</sup> as the tube temperature rises ( $N \sim 1/T$ ). At higher temperatures diffusion losses of electrons to the walls become dominant and the electron density is reduced. As the CuCl vapor pressure becomes about 1% of the total pressure, the Cu and Cl atoms with their lower ionization potentials contribute heavily to the electron population, thereby increasing the electron density.

The same discharge tube was used as a Cu/CuCl laser. The excitation load was changed to a double-pulse arrangement<sup>12</sup> operated at 12.5 kV and employing

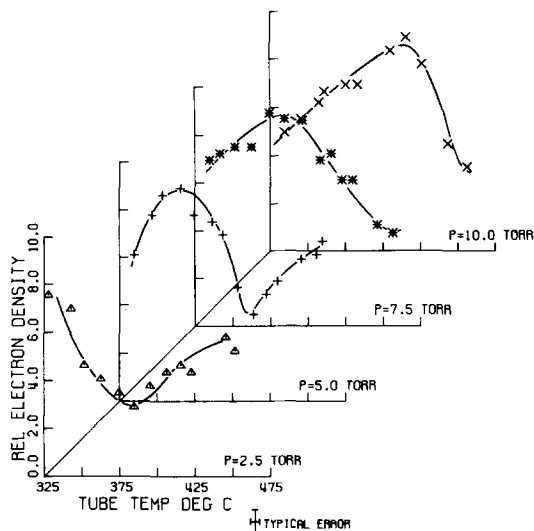


FIG. 1. Electron densities in a pulsed CuCl/Ne discharge. With increasing pressure, both the minimum and maximum in the electron density shift to higher temperature.

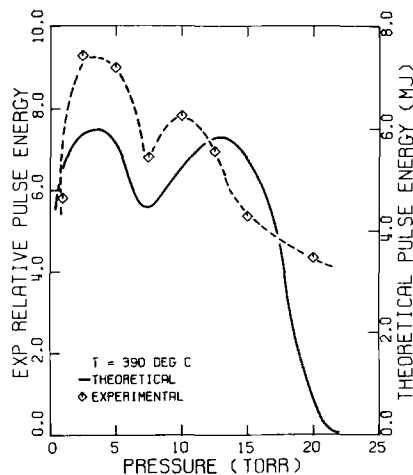


FIG. 2. Experimental and computed results for laser-pulse energy at a tube temperature of 390/C. The experimental scale was chosen for ease of comparison.

14.4-nF dissociation and 14.4-nF pumping capacitors. The laser-pulse energy was optimized with respect to the time delay between dissociation and pumping pulses. A photodiode was used to measure the optical-pulse energy. For experimental convenience, the tube temperature was held constant and the Ne pressure was varied. The results for a tube temperature of 390°C are shown in Fig. 2. The laser-pulse energy reaches a maximum at low gas pressure, shows a local minimum as the pressure is increased, and then declines to low values at higher buffer-gas pressure. As shown in Fig. 3, a correlation can be made between the extrema in electron density and the extrema in laser-pulse energy. When plotted as a function of tube temperature, the pressures at which the electron density is locally minimum and laser-pulse energy is maximum fall approximately on a straight line. Similar behavior was found for the pressures at which the electron density is a local maximum and laser-pulse energy a local minimum. This correlation between maximum laser output energy and minimum electron density has also been made with the positive-column He-Cd\* laser.<sup>13</sup>

These results, when combined with the results of the electron temperature measurements,<sup>7</sup> suggest the following interpretation. At higher electron densities ( $n_e \approx 2 \times 10^{14}/\text{cm}^3$ ) and correspondingly high electron temperatures ( $T_e \approx 15$  eV), the copper ionization rates from both ground state and excited levels exceed the excitation rates to the upper laser levels. The laser-pulse energy is therefore depressed because there is less ground-state copper available to pump to the upper level. Charge exchange with neon ions and Penning ionization with neon metastables during the afterglow between dissociation and pumping pulses will also contribute to the depletion of ground-state copper. Due to the high ionization potential (21.6 eV) and metastable energy (16.7 eV) of neon, these affects will be important only at the higher electron temperatures referred to above. As the electron density and electron temperature decrease, the ionization rates are reduced, leaving more ground-state copper, and the excitation rates are increased. At these electron temperatures ( $T_e \sim 10$  eV), the electron distribution is maximum near

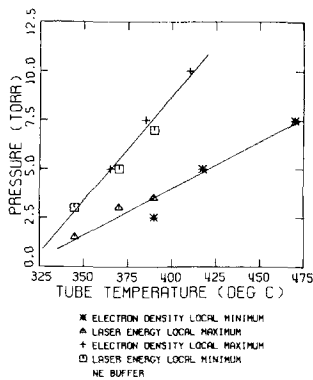


FIG. 3. When plotted as a function of tube temperature, pressures at which electron density is a minimum and laser energy is a maximum fall on a straight line. The same is true for electron density maximum and laser energy minimum.

the peak of the resonance-impact cross section for excitation to the upper laser levels.<sup>14,15</sup> Under these conditions, laser-pulse energy is a maximum. At low electron densities ( $n_e \leq 5 \times 10^{13}$ ) and temperatures ( $T_e \approx 5$  eV), the ionization rate is reduced significantly so that there is an abundance of copper atoms available for excitation, but because the optimum electron temperature for excitation to the upper laser level occurs at higher values while the excitation rate to the lower laser level is becoming larger, the net excitation rate is lowered and the laser pulse energy is also small.

With the above interpretation as a basis, a set of rate equations have been constructed for the copper laser. Five equations are used for the populations of three copper atom levels and two neon levels; the sixth equation governs the optical-pulse intensity. As a simplification, the populations of CuCl and Cl are not considered. Semiempirical cross sections for the excitation of copper<sup>14,15</sup> and an experimental electron distribution function<sup>16</sup> are used. The value of the electron density at the peak of the discharge current pulse was specified for each tube temperature and buffer-gas pressure in accordance with the experimental results reported here. The assumption is made that the electron temperature is constant for a given tube temperature and pressure and directly proportional to the peak electron density. The rate equations have been integrated over a 100-ns-wide parabolic current pulse using the Runge-Kutta-Gill method with Adams-Moulten correction features.<sup>17</sup> Typical results for one set of experimental conditions are shown in Fig. 2.

These results reproduce the observed extrema in laser energy. Gryzinski cross sections<sup>18</sup> were initially used for copper ionization rates, but it was found that the peak value of these cross sections had to be increased by at least a factor of 3 in order to obtain the results displayed. The behavior observed at high pressures ( $p > 10$  Torr) is not represented well. In particular, the second maximum in laser energy is displaced to higher pressures and the value of the second maximum is too high, being nearly equal to that of the first. This discrepancy may be partly due to the difference at higher pressures between the CuCl discharge, which provide the values for the electron density, and the double-pulsed discharge used for the laser.

Because the differences are greater at high pressure, one would expect that processes involving the buffer gas

may be responsible for the reduced optical-pulse energy. With this in mind, Penning ionization rates ( $\text{Ne}^* + \text{Cu} \rightarrow \text{Ne} + \text{Cu}^* + e$ ) and the initial fraction of metastable neon were varied in the model. A Penning cross section of  $5 \times 10^{-15}$  cm<sup>2</sup> and initial metastable fractions of 0.1 were required in order to reduce the high-pressure optical-pulse energy to experimental values. The relative influence of the slower atom-atom interaction rates on the optical-pulse energy is small because the laser pulse occurs in the first 40 ns of the current pulse. The laser pulse is over before the population of excited neon has reached maximum. It appears that one must look to atom-atom processes occurring in the relatively long afterglow between the dissociation pulse and the pumping pulse to explain the high-pressure behavior.

In summary, electron densities have been measured in a CuCl/Ne discharge using a CO<sub>2</sub> laser interferometer. Local maximum and minimum values of electron density were found to move to higher tube temperature at higher buffer pressures. The maximum values of electron density were found to correlate with minimum values of pulse energy from a double-pulse Cu/CuCl laser. Minimum values of electron density were found to correlate with maximum values of pulse energy. An analysis based on rate equations using experimental values of electron density and temperature as input data reproduced the extrema in the pulse energy. This agreement between calculated and experimental results supports the proposition that ionization of copper is a dominant mechanism in reducing the pulse energy for a double-pulsed Cu/CuCl laser operated at tube temperatures greater than the optimum value.

This work was supported by grant PF-083 from the President's Fund, California Institute of Technology. The experiments were performed at the Jet Propulsion Laboratory. The authors especially are indebted to Noble Nerheim for his initial and continuing advice throughout the program. The authors wish also to thank Robert Chapman and George Alahuzas for their technical assistance.

<sup>1</sup>C. J. Chen, N. M. Nerheim, and G. R. Russell, *Appl. Phys. Lett.* **23**, 514 (1973).

<sup>2</sup>J. Tenenbaum, I. Smilanski, S. Gabay, G. Erez, and L. A. Levin, *J. Appl. Phys.* **49**, 2662 (1978).

<sup>3</sup>I. Liberman, R. V. Babcock, C. S. Liu, T. V. George, and L. A. Weaver, *Appl. Phys. Lett.* **25**, 334 (1974).

<sup>4</sup>W. T. Walter, N. Solimene, M. Piltch, and G. Gould, *IEEE QE-2*, 474 (1966).

<sup>5</sup>R. S. Anderson, L. W. Springer, B. G. Bricks, and T. W. Karras, *IEEE J. Quantum Electron.* **QE-11**, 173 (1975).

<sup>6</sup>N. M. Nerheim, *J. Appl. Phys.* **48**, 1186 (1977).

<sup>7</sup>E. Sovero, C. J. Chen, and F. E. C. Culick, *J. Appl. Phys.* **47**, 4538 (1976).

<sup>8</sup>J. B. Gerardo and J. T. Verdeyen, *Proc. IEEE* **52**, 690 (1964).

<sup>9</sup>J. B. Gerardo, J. T. Verdeyen, and M. A. Gusinow, *J. Appl. Phys.* **36**, 2146 (1965).

<sup>10</sup>The tube temperature was measured with a Chromel/Alumel thermocouple at the midpoint between electrodes on the outer tube surface.

<sup>11</sup>S. C. Brown, *Basic Data of Plasma Physics*, (MIT/Wiley, New York, 1959), p. 134.  
<sup>12</sup>A. A. Vetter, *IEEE J. Quantum Electron.* **QE-13**, 380 (1967).  
<sup>13</sup>T. Goto, A. Kawahara, G. J. Collins, and S. Hattori, *J. Appl. Phys.* **42**, 3816 (1971).  
<sup>14</sup>D. A. Leonard, *IEEE J. Quantum Electron.* **QE-3**, 380 (1967).

<sup>15</sup>S. Trajmar, W. Williams, and S. K. Srivastava, *J. Phys.* **B 10**, 3323 (1977).  
<sup>16</sup>R. H. Bond, Ph.D. thesis, California Institute of Technology, 1965.  
<sup>17</sup>K. Matsumoto, California Institute of Technology Computer Center Library (unpublished).  
<sup>18</sup>M. Gryzinski, *Phys. Rev.* **138**, A336 (1965).

## Dichromatic switching effect in two thin-film DFB dye lasers

A. Matsuda and S. Izima

*Electrotechnical Laboratory, Tanashi, Tokyo, Japan*  
 (Received 26 June 1978; accepted for publication 24 July 1978)

Interaction between two thin-film DFB dye lasers which are excited simultaneously in the same film plane has been investigated. A dichromatic switching effect of one of the lasers caused by the on and off switching of the excitation of another laser has been observed and an adequate model for the effect has been discussed.

PACS numbers: 42.60.Fc, 42.80.Lt, 42.80.Sa

The distributed feedback (DFB) laser has been investigated<sup>1-3</sup> as the light source of an integrated optical circuit. Modulation of the laser beam in the thin-film waveguide has been required for the optical communication system. Most methods published so far for modulating the light beam in the thin film use the variation of the parameters of the material of the thin film by electro-optical, acousto-optical, magneto-optical, or photo-optical means.<sup>4,5</sup> This paper describes the interaction between two DFB lasers which are excited simultaneously in the same film and show the possibility of modulation of the light beam by the direct action of another light beam.

Figure 1 shows the experimental setup for the observation of the interaction between two thin-film dye lasers. Two DFB dye lasers having different wavelengths are constructed in the same organic film by the technique which was previously published by the authors.<sup>6</sup> Each DFB laser is pumped by a N<sub>2</sub> laser beam (Lambda Physik K300; 100 kW). The dye-laser beams generated in DFB regions are propagated to the right and left in the film. The wavelength and intensity of the propagated laser beams are observed at scratches A and B made on the film using an optical multichannel analyzer (OMA) through an optical fiber whose one end is fixed at the scratch and the other end is put into the OMA system.

When only laser *a* is excited by the N<sub>2</sub> laser, light with wavelength  $\lambda_a$ , which is characteristic of laser *a*,

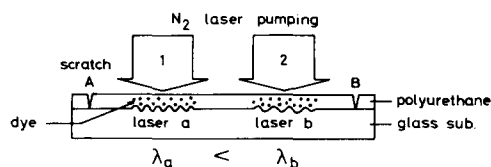


FIG. 1. Experimental setup for observing the interaction of two DFB lasers (lasers *a* and *b*).

is observed at point A, as shown on the left-hand side of Fig. 2(a). When lasers *a* and *b* are excited simultaneously by the N<sub>2</sub> laser, light with  $\lambda_a$  decreases and strong light with wavelength  $\lambda_b$ , which is characteristic of laser *b*, is observed at point A as shown on the left-hand side of Fig. 2(b). Namely, when laser *b* is switched on, the main peak of the laser spectrum observed at point A is converted from  $\lambda_a$  to  $\lambda_b$ ; thus, the dichromatic switching takes place. On the other hand, if the observing point is changed from A to B, the dichromatic switching from  $\lambda_b$  to  $\lambda_a$  occurs by the switching on of the excitation of laser *a* as shown in the right figure of Fig. 2.

The period of grating was varied from 1813 to 2000 Å. The corresponding wavelength of the lasers ranged from 5800 to 6400 Å. A super-radiation whose center of wavelength is located at about 6030 Å is observed by N<sub>2</sub> laser irradiation at the no-grating region on the sample. It should be noted here that a clear dichromatic switching

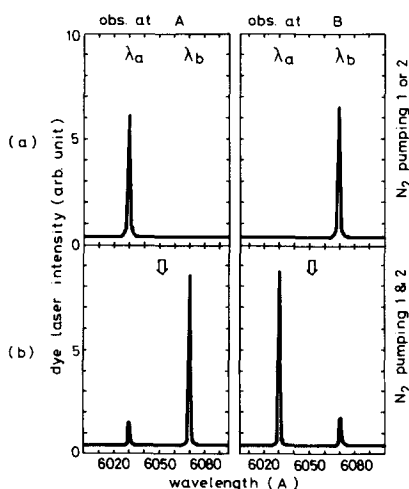


FIG. 2. Observed wavelength and intensity at points A and B when (a) the N<sub>2</sub> laser excitation 1 or 2 is on and (b) when N<sub>2</sub> laser excitations 1 and 2 are on.